Supplement: Consensus based odour source localisation by multiagent systems

Abhinav Sinha, Ritesh Kumar, Rishemjit Kaur and Amol P. Bhondekar

Abstract

This paper presents an investigation of the task of localising unknown source of an odour by heterogeneous multiagent systems. A hierarchical cooperative control strategy has been proposed as a potential candidate to solve the problem. The agents are driven into consensus as soon as the information about the location of source is acquired. The controller has been designed in a hierarchical manner of group decision making, agent path planning, and robust control. In group decision making, Particle Swarm Algorithm has been used along with the information of the movement of odour molecules to predict the odour source location. Next, a trajectory has been mapped using this predicted location of source, and the information is passed to the control layer. A variable structure control has been used in the control layer due to its inherent robustness and disturbance rejection capabilities. Cases of movement of agents towards the source under consensus, and parallel formation have been discussed. The efficacy of the proposed scheme has been confirmed by simulations.

Index Terms

Odour source localisation (OSL), robot olfaction, heterogeneous multiagent systems (MAS), inverse sine hyperbolic reaching law, sliding mode control, decentralised cooperative control.

This supplement provides some additional illustrations to aid the propositions made in the manuscript entitled "*Consensus based odour source localisation by multiagent systems*" concerned with localisation of a stationary odour source by multiagent systems in a turbulent environment.

I. Wind turbulence in the domain

The domain of localisation is characterised by heavy turbulence. Hence, we have taken snapshots in different segments of time to illustrate the turbulence using velocity plots. Figure 1 depicts wind turbulence in the domain during consensus based localisation. In each 2.5 second window, a random snapshot of airflow is taken. Here, we illustrate four such snapshots for consensus based localisation (figure 1) and another four snapshots for formation based localisation (figure 2). The first snapshot is taken randomly between $0 < t < 2.5$ sec and the velocity plot depicting turbulence at that time has been presented. In a similar way, other snapshots have been taken for other time segments. Length of the arrows in the velocity plots (figures 1 and 2) represent the magnitude of the wind velocity, and the direction of arrows correspond to the direction of wind. It is evident from the plots that in spite of near uniform airflow velocity in the domain, there are irregular fluctuations in the direction of wind leading to statistical variations in the flow.

II. Localisation in $\mathbb{R}^1$ and $\mathbb{R}^2$

For the case of $\mathbb{R}^1$, the odour source is randomly placed between 10 m and 11 m, as shown in figure 3. Agents and their respective trajectories are represented by five different colours. The odour source is represented by a grey circle, and the filaments released from the odour source are represented as black dots. Agents start from various initial conditions that are far from the origin. Agents start moving from left hand side to progress towards the source via instantaneous plume sensing (by sensing odour molecules, or filaments). As soon as the leader agent senses the odour molecules, the information of predicted next state is exchanged among other agents. This local information is then used to make a consensus while localisation. It is evident that agents come to consensus in finite time to locate the odour source. In spite of time varying disturbance, the plume tracking is accurate and the localisation is successful. In figure 4, agents locate the odour source in parallel formation. During parallel formation, a fixed distance is maintained between two consecutive agents. In both the cases, filaments or odour molecules (source information) are released from the odour source and are detected by the sensors equipped with the agents.

A. Sinha is with Indian Institute of Technology, Bombay (Mumbai), India. He was with School of Mechatronics & Robotics, Indian Institute of Engineering Science and Technology; and Central Scientific Instruments Organisation (CSIR–CSIO), India. **email:** sinha.abhinav@iitb.ac.in. **ORCiD:** 0000–0001–6419–2353 (A. Sinha).
R. Kumar, R. Kaur & A. P. Bhondekar are with CSIR–CSIO. **emails:** riteshkr@csio.res.in, rishemjit.kaur@csio.res.in, amolbhondekar@csio.res.in.

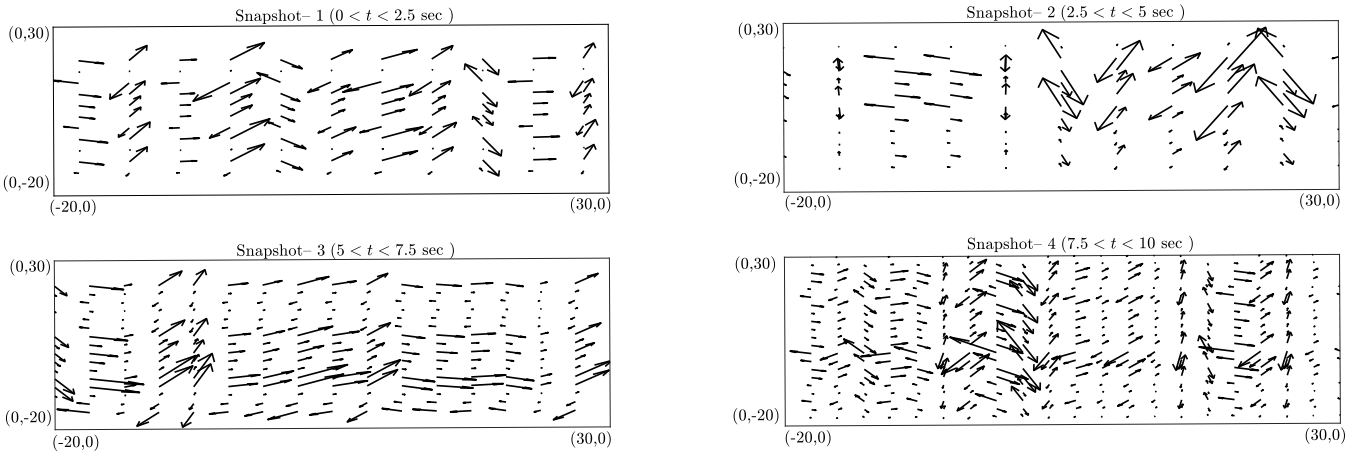

Fig. 1: Wind turbulence in the domain during consensus based localisation.

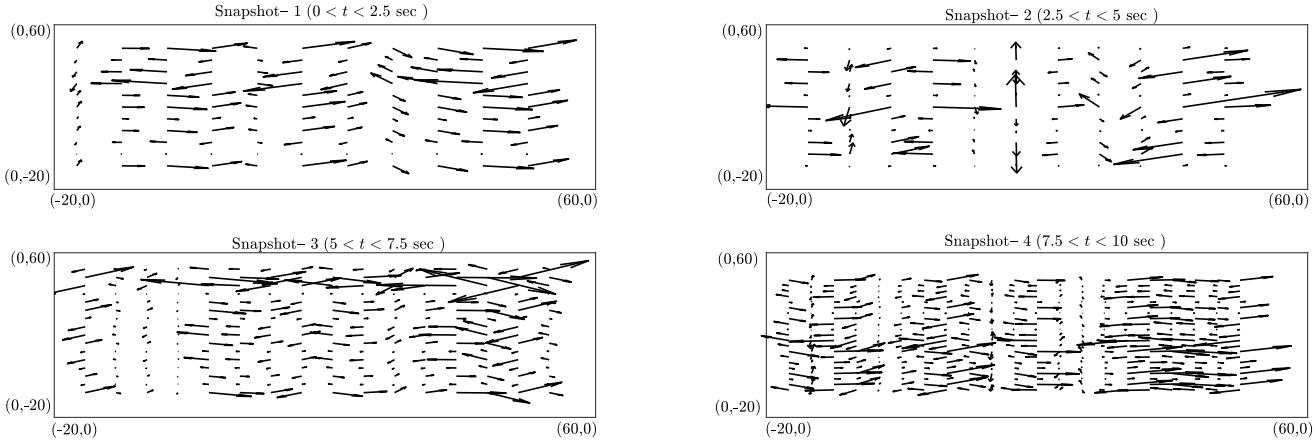

Fig. 2: Wind turbulence in the domain during formation based localisation.

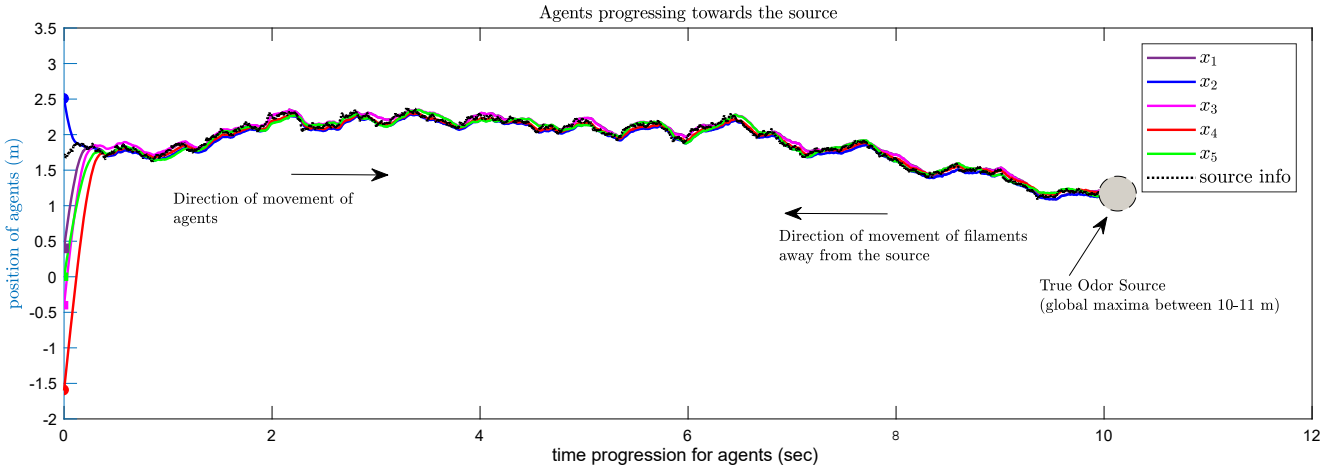

Fig. 3: Agents in consensus to locate source of odour in $\mathbb{R}^1$.

Although the filaments disperse throughout the domain, only the source information relevant to the agents has been shown in the figures. Agents start from left and progress towards the source to the right.

Similarly, figures 5 and 6 correspond to localisation in $\mathbb{R}^2$. Two best case scenarios have been presented to illustrate the efficacy of the proposed scheme. Figure 5 shows consensus based localisation in $\mathbb{R}^2$. Figure 6 shows agents making parallel formation in $\mathbb{R}^2$ to locate the source (domain of localisation is defined via axis limits, which happens to be a grid of 80×80). In the formation case, abscissa and ordinate range from -20 to 60. The explanation is similar to that for the case of consensus based localisation.

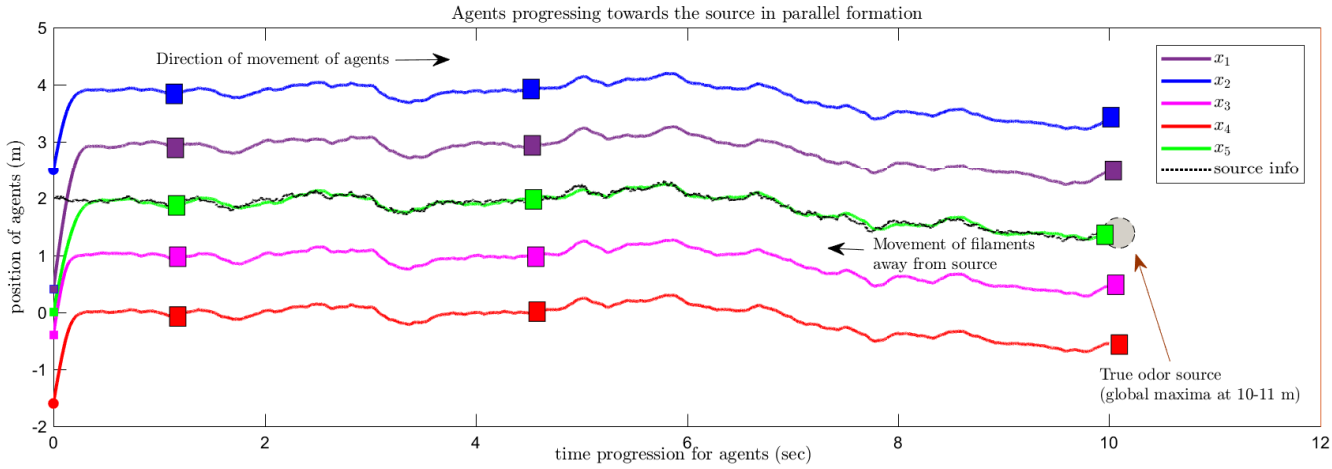

Fig. 4: Agents in formation to locate source of odour in $\mathbb{R}^1$.

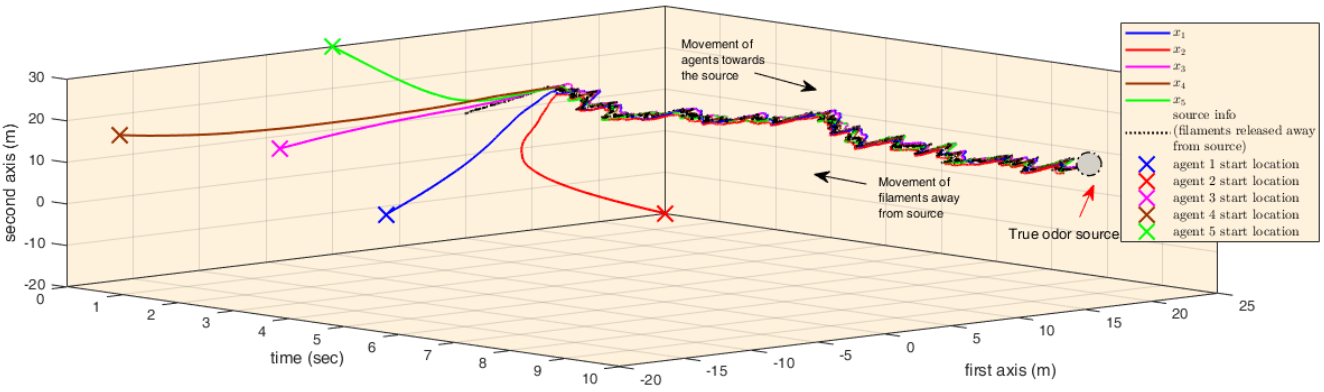

Fig. 5: Agents in consensus to locate source of odour in $\mathbb{R}^2$.

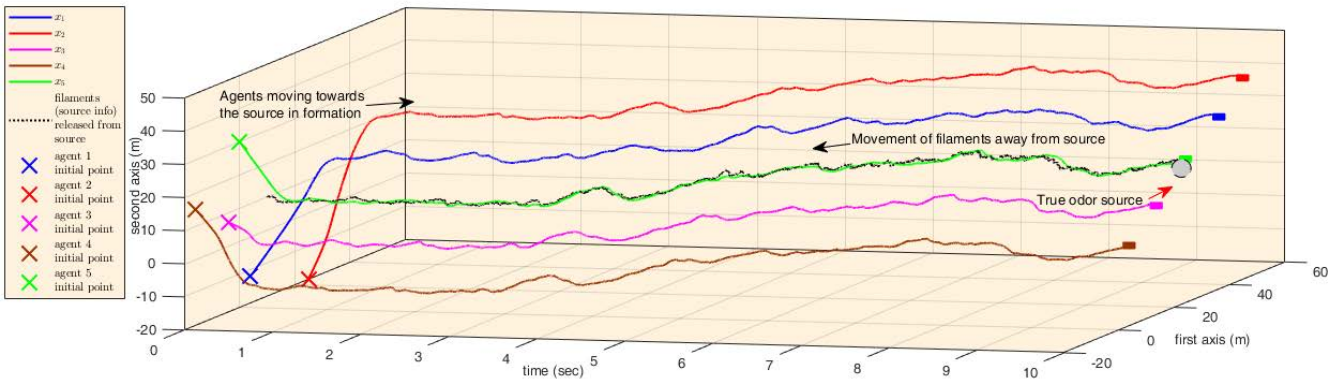

Fig. 6: Agents in formation to locate source of odour in $\mathbb{R}^2$.

III. Reaching time under the influence of forcing function

The time required by the state trajectories (t_r) to reach the sliding manifold can be calculated as follows:

$$\because \quad \dot{s}_i(t) = -\mu \sinh^{-1}(m + w|s_i(t)|)sign(s_i(t)),$$

$$\therefore \quad -\mu \; sign(s_i(t))dt = \frac{ds_i(t)}{\sinh^{-1}(m + w|s_i(t)|)}.$$

$$\Rightarrow \int_0^{t_r} dt = \frac{1}{\mu} \int_0^{s_i(0)} \frac{sign(s_i(t))}{\sinh^{-1}(m + w|s_i(t)|)} ds_i(t) \tag{1}$$

For $sign(s_i(t)) > 0$, we have

$$\int_0^{t_r} dt = \frac{1}{\mu}\int_0^{s_i(0)} \frac{ds_i(t)}{\sinh^{-1}(m + w|s_i(t)|)}. \tag{2}$$

For $sign(s_i(t)) < 0$, we have

$$\begin{aligned}\int_0^{t_r} dt &= -\frac{1}{\mu}\int_0^{s_i(0)} \frac{ds_i(t)}{\sinh^{-1}(m + w|s_i(t)|)} \\ &= \frac{1}{\mu}\int_0^{-s_i(0)} \frac{ds_i(t)}{\sinh^{-1}(m + w|s_i(t)|)}.\end{aligned} \tag{3}$$

From $(2-3)$, the results can be combined as

$$\int_0^{t_r} dt = \frac{1}{\mu}\int_0^{|s_i(0)|} \frac{ds_i(t)}{\sinh^{-1}(m + w|s_i(t)|)} \tag{4}$$

which can be further simplified as

$$t_r = \frac{1}{\mu}\int_0^{|s_i(0)|} \frac{ds_i(t)}{\sinh^{-1}(m + w|s_i(t)|)}. \tag{5}$$

$$\therefore \quad t_r = \frac{1}{\mu w}\Big(\chi\big(\sinh^{-1}(m + w|s_i(0)|)\big) - \chi\big(\sinh^{-1}(m)\big)\Big) \tag{6}$$

where $\chi(\cdot)$ denotes the $cosh\ integral$ function. By definition,

$$\chi[z] = \gamma + Ln[z] + \int_0^z \frac{cosh(t) - 1}{t} dt \tag{7}$$

with $\gamma = 0.577216$ as the Euler's constant.

$$\text{Thus,} \qquad t_r \propto \frac{1}{\mu w}. \tag{8}$$

Hence, higher the gain parameters, lesser the convergence time.